Lawrence Berkeley Laboratory
UNIVERSITY OF CALIFORNIA, BERKELEY, CA

Physics, Computer Science & Mathematics Division

To be presented at the VIth International Symposium on Combustion Processes, Karpacz, Poland, August 26-30, 1979

A HYBRID RANDOM CHOICE METHOD WITH APPLICATION TO INTERNAL COMBUSTION ENGINES II

Gary A. Sod

June 1979

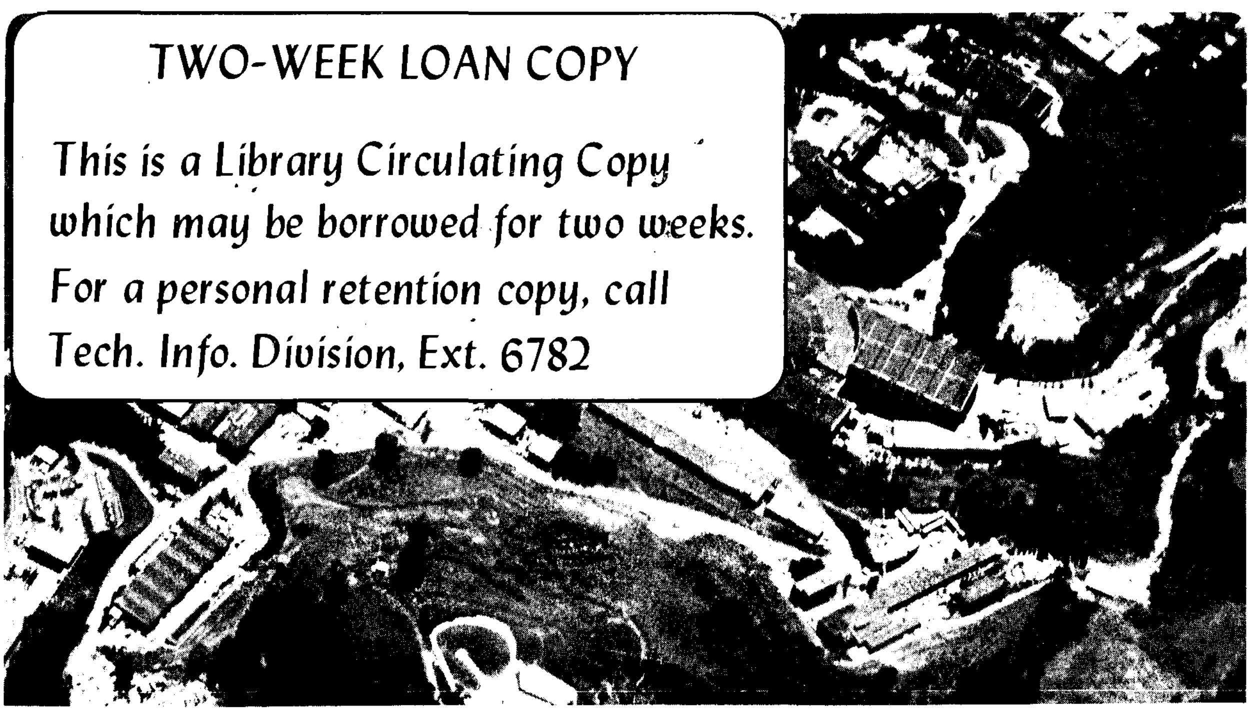

Prepared for the U. S. Department of Energy
under Contract W-7405-ENG-48

DISCLAIMER

A Hybrid Random Choice Method With Application to Internal Combustion Engines II

Gary A. Sod*

Mathematics Research Center
University of Wisconsin
Madison, Wisconsin 53706

and

Lawrence Berkeley Laboratory
University of California
Berkeley, California 94720

Abstract. A numerical procedure was introduced for solving one-dimensional equations of gas dynamics for a cylindrically or spherically symmetric flow. This method has been generalized to the two-dimensional equations of gas dynamics in a cylindrical geometry. This is coupled at the boundary with a new grid free method for introducing viscous effects, where the computational elements are segments of vortex sheets and circular vortex filaments. Examples are given for flow in a motored engine chamber during intake and compression strokes.

*Supported in part by the Sloan Foundation and the Department of Energy under Contract No. EY-76-C-02-3077 at the Courant Institute of Mathematical Sciences and the Department of Energy under Contract No. W-7405-Eng-48 at Lawrence Livermore Laboratory and Lawrence Berkeley Laboratory.

Introduction. Recently a numerical procedure was introduced for solving the one-dimensional equations for an inviscid, radially symmetric flow [1] and [2]. The idea of the method was to use operator splitting to reduce this system of equations to two systems of equations; the equations of gas dynamics in Cartesian coordinates and a system of simultaneous ordinary differential equations. This method has been generalized to treat the two-dimensional equations of gas dynamics for an inviscid fluid in a cylindrical geometry.

When considering the flow in the cylinder of an internal combustion engine viscous effects cannot be ignored. The effect of viscosity in two-dimensions is confined to regions near the boundaries. Viscosity results in the creation of a thin boundary layer, which later separates into the fluid.

A grid free method for approximating the incompressible boundary layer equation for a cylinder and a flat plate is used. The computational elements are pieces of vortex sheets [3] and vortex filaments [4]. The desirability of a grid free method can be seen from analysis which implies that if a grid method is used then several grid points must fall within the boundary layer whose thickness is $O(R^{-1/2})$, where R is the Reynolds number. Thus a relatively low upper bound must be imposed on the Reynolds number. In the problem considered below R, ranges from 1000 to 10000.

The computational domain is divided into two regions, one the interior and the other the region near the boundary. Different assumptions about compressiblity are made, as well as different numerical methods used, in the two regions. Near the boundary the flow will be considered viscous and incompressible and in the interior the flow will be considered inviscid and compressible. A new way of coupling the two methods which greatly reduces the number of segments of vortex sheets needed will be discussed in a later section.

1. Outline of the Method for Interior. The two-dimensional equations for an inviscid, non-heat conducting flow in cylindrical coordinates with axial symmetry and zero azimuthal velocity can be written in the form

$$\partial_t \underline{U} + \partial_r \underline{F}(\underline{U}) + \partial_z \underline{G}(\underline{U}) = -\frac{1}{r}\underline{W}(\underline{U}), \qquad (1)$$

where

$$\underline{U} = \begin{pmatrix} \rho \\ \rho u_r \\ \rho u_z \\ e \end{pmatrix}, \quad \underline{F}(\underline{U}) = \begin{pmatrix} \rho u_r \\ \rho u_r^2 + p \\ \rho u_r u_z \\ (e+p) u_r \end{pmatrix}, \quad \underline{G}(\underline{U}) = \begin{pmatrix} \rho u_z \\ \rho u_r u_z \\ \rho u_z^2 + p \\ (e+p) u_z \end{pmatrix}$$

and

$$\underline{W}(\underline{U}) = \begin{pmatrix} \rho u_r \\ \rho u_r^2 \\ \rho u_r u_z \\ (e+p) u_r \end{pmatrix},$$

where ρ is the density, u_r is the velocity in the radial direction, u_z is the velocity in the axial direction, p is the pressure, e is the energy per unit volume, t is time, and r is the radial distance from the axis of symmetry. We may write

$$e = \frac{p}{\gamma - 1} + \frac{1}{2} \rho (u_r{}^2 + u_z{}^2)$$

holding for a polytropic gas, where γ is the ratio of specific heats (a constant greater than 1).

There are several major problems involved in solving the system (1) directly the first is the singular term near the axis ($r = 0$), that is, there are singular terms proportional to $\frac{1}{r}$. The second problem is that the momentum equations (the second and third component equations of (1)) cannot be put into conservation form. These problems cause major difficulties near the axis.

In the method developed by the author [1] and [2] for one-dimensional flows and extended here to two-dimensional flows, both problems have been removed without having to resort to any ad-hoc method.

The first step is to use operator splitting to remove the inhomogeneous term $-\frac{1}{r} \underline{W}(\underline{U})$ from the system (1). The resulting set of equations takes the form

$$\partial_t \underline{U} + \partial_t F(\underline{U}) + \partial_z G(\underline{U}) = 0, \qquad (2a)$$

$$d_t\underline{U} = -\frac{1}{r}\underline{W}(\underline{U}). \tag{2b}$$

The system of equations (2a) represents the two-dimensional equations of gas dynamics in Cartesian coordinates, written in conservation form.

The method used to solve system (2a) is the random choice method introduced By Glimm [5] and developed for hydrodynamics by Chorin [6].

Consider the nonlinear system of equations

$$\partial_t\underline{U} + \partial_x\underline{F}(\underline{U}) = 0. \tag{3}$$

The random choice method (Glimm's method) is outlined as follows.

Divide time into intervals of length Δt and let Δx be the spatial increment. The solution is to be evaluated at time $n\Delta t$ where n is a nonnegative integer at the spatial points $i\Delta x$, where $i = 0, \pm 1, \pm 2, \ldots$ and at time $(n + \frac{1}{2})\Delta t$ at $(i + \frac{1}{2})\Delta x$. This is a two step method. Let $\underline{u}_i^n$ approximate $\underline{U}(i\Delta x, n\Delta t)$ and $\underline{u}_{i+\frac{1}{2}}^{n+\frac{1}{2}}$ approximate $\underline{U}((i + \frac{1}{2})\Delta x, (n + \frac{1}{2})\Delta t)$. To find the solution $\underline{u}_{i+\frac{1}{2}}^{n+\frac{1}{2}}$ given $\underline{u}_i^n$ and $\underline{u}_{i+1}^n$, consider the system (4) along with the piecewise constant initial date

$$\underline{U}(x,n\Delta t) = \begin{cases} \underline{u}_{i+1}^n, & x > (i + \frac{1}{2})\Delta x, \\ \underline{u}_i^n, & x < (i + \frac{1}{2})\Delta x. \end{cases}$$

This defines a sequence of Riemann problems. If $\Delta t < \frac{\Delta x}{(|u| + c)}$, where c is the local sound speed, the waves generated by the individual Riemann problems will not interact. Hence the solution $\underline{v}(x,t)$ to the Riemann problems can be combined into a single exact solution. Let ξ_n be an equidistributed random variable which is given by the Lebesque measure on the interval $(-\frac{1}{2}, \frac{1}{2})$. Define

$$\underline{u}_{i+\frac{1}{2}}^{n+\frac{1}{2}} = \underline{v}((i + \frac{1}{2} + \xi_n)\Delta x, (n + \frac{1}{2})\Delta t). \tag{4}$$

At each time step, the solution is approximated by a piecewise constant function. The solution is then advanced in time exactly and the new values are sampled. The method depends on being able to solve the Riemann problem exactly and inexpensively. The Riemann problem can be efficiently solved by an iterative method due to Godunov [7] and modified by Chorin [6]. As indicated in the review by the author [8], this iterative procedure made the Glimm scheme above $2\frac{1}{2}$ times slower per grid point than most finite difference schemes. A modification in the iterative procedure by the author [9] makes this random method comparable timewise with most finite difference schemes.

The generalization of Glimm's methods to two space dimensions is done by operator splitting. Thus equation (2a) can be written as two sets of one dimensional equations of the form of (3). The two systems of one dimensional equations are solved on a staggered grid in order to ensure consistency. A single two dimensional time step consists of four quarter steps. Each is a sweep in the z or r direction.

Glimm's method will produce perfectly sharp shocks and contact discontinuities. However, for multidimensional problems there are oscillations in a neighborhood of the shocks. This is a dispersive effect due to the operator splitting (used to reduce the number of space dimensions). This is usually not observed in finite difference methods due to the truncation error and the inclusion of artificial viscosity which smooths such oscillations. A numerical study demonstrating this property has been conducted by Colella [10].

To reduce these oscillations an artificial viscosity term is added at each quarter step. The form is a modified version of the artificial viscosity considered by Lapidus [11]. See Colella [10] and Sod [9] and [12] for specialization to Glimm's scheme.

Once the solution of system (2a) $\tilde{u}_{i,j}^{n+1}$ is obtained, we must solve a system of ordinary differential equations (2b). We approximate equation (2b) by a modified version of the Cauchy-Euler scheme. Randomness, in keeping with the spirit of the Glimm scheme, is introduced which was not in the original method. See Sod [1].

Let ξ_1 and ξ_2 be the random variables used in the two r-sweeps. Then system (2b) is approximated by

$$u_{i,j}^{n+1} = \underline{u}_{i,j}^{n} = \frac{\Delta t}{(i + \xi_1 + \xi_2)} \underline{W}(\underline{\tilde{u}}_{i,j}^{n+1}). \tag{5}$$

Originally r in system (2b) was replaced with $i\Delta r$, here r is replaced with $(i + \xi_1 + \xi_2)\Delta r$. At the end of the two r-sweeps the place at which the solution is found is offset from the grid point $i\Delta r$ by $(\xi_1 + \xi_2)\Delta r$. This gives the solution of (2b) which is in phase with the solution of (2a) in the r-direction.

Since the sampling used is the stratified sampling as developed by Chorin [6], the values of ξ_1 and ξ_2 are never such that $i + \xi_1 + \xi_2 = 0$.

2. Boundary Layer Treatment. Consider the flow past a circular cylinder of constant radius r_0 parallel to its axis $(r = 0)$. A boundary layer, initially of zero thickness, is formed on the surface of the cylinder. The Prandtl boundary layer equations for a semi-infinite flat plate are a valid approximation. The boundary layer grows parabolically in thickness with increasing z. A stage will be reached when the thickness of the boundary layer can no longer be neglected compared with r_o. So for a long axially symmetric cylinder, the boundary layer equations for a flat plate break down. Certain derivatives in r may no longer be neglected. See Schlichting [13].

The boundary layer equations for axially symmetric cylinder (retaining the correct derivatives in r) may be written in the form

$$\partial_t \xi + (\underline{u} \cdot \underline{\nabla}) \xi = \partial_r^2 \xi + \frac{\nu}{r} \partial_r \xi, \tag{6a}$$

$$\partial_z (r u_z) + \partial_r (r u_r) = 0, \tag{6b}$$

$$\xi = - \partial_r u_z, \tag{6c}$$

where $\underline{u} = (u_z, u_r)$ with u_z tangent to the boundary and u_r normal to the boundary ξ is the vorticity, and ν is the viscosity. The boundary conditions are

$$\underline{u}(r_0, z) = 0,$$

$$\underline{u}(\infty, z) = U_\infty(z).$$

We integrate equation (6c) to obtain the tangential component of velocity

$$u_z(r,z) = U_\infty(z) - \int_r^\infty \xi(r,t)\,dr. \tag{7a}$$

With this equation (6b) may be integrated to obtain the normal component of the velocity

$$u_r(r,z) = -\frac{1}{r}\,\partial_z \int_{r_0}^{r} r u_z(r,z)\,dr, \tag{7b}$$

which is nonsingular provided $r_0 > 0$. Hence once the vorticity $\xi(r,z)$ is known the velocity field in the boundary layer may be obtained.

The method used is one introduced by Chorin [3] for the boundary layer equations for a flat plate in two-dimensions. Consider a collection of N segments S_i of vortex sheets with intensities ξ_i, $i = 1, \ldots, N$. The S_i are straight line segments parallel to the z-axis having length h and center (r_i, z_i). The tangential velocity u_{z_i} of S_i due to the presence of the other segments is obtained by approximating (7a). The normal velocity u_{r_i} of S_i due to the presence of the other segments is obtained by approximating (7a). The normal velocity u_{r_i} of S_i due to the presence of the other segments is obtained by approximating (7b).

Consider the semi-infinite strip $R_i = \{(r, z) \mid r \geq r_0 \text{ and } z_i - h/2 \leq z \leq z_i + h/2\}$. The number of interactions among the segments is small since for a segment S_j to influence a given segment S_i it must intersect the strip R_i.

Operator splitting is used to write equations (6a-c) in the form

$$\partial_t \xi + (\underline{u}\cdot\underline{\nabla})\xi = 0,$$

$$\partial_z(ru_z) + \partial_r(ru_r) = 0, \tag{8}$$

$$\xi = -\partial_r u_z,$$

$$\partial_t \xi - \frac{\nu}{r}\,\partial_r \xi = 0, \tag{9}$$

and

$$\partial_t \xi = \nu \partial_r^2 \xi. \tag{10}$$

System (8) is solved deterministically where the sheets S_i are advanced in time according to the tangential (u_{z_i}) and normal (u_{r_i}) components of velocity. Equation (9) is responsible for diffusing the sheets in the r-direction. This equation solved by a random walk. Finally, the sheets are moved along the characteristics of equation (10).

For further details as well as a discussion of the method of vorticity creation see Chorin [3] and [14] and Sod [9], [12], and [15].

3. Coupling of Interior and Boundary Layer Methods. Finally we must describe how the two methods are pieced together. The method used to couple the boundary layer calculation to the interior calculation is more complicated than originally considered by Chorin [3].

It is essential that the boundary layer act on the interior (unless the boundary layer does not separate). In this method the edge of the calculation is not the boundary of the domain, but rather the edge of the boundary layer.

In the problem considered below the boundary is substantially more complicated than a simple cylinder. We shall allow for boundaries which consist of pieces of cylinders and flat plates (normal to cylinder). The boundary layer equations for a flat plate are used for these regions normal to the cylinders.

A boundary layer calculation for the entire boundary is made every two quarter steps each with time step $\frac{\Delta t}{2}$. The tangential component of the velocity at the edge of the interior calculation (edge of the boundary layer) is used as the velocity at infinity for the boundary layer calculation. For the boundary layer calculation the velocity at infinity is considered to be piecewise constant over the same intervals as in the interior calculation. This is important since the values of r and z in the interior calculation may not be the same as the spacing h of the boundary points for the boundary layer calculation.

In an earlier version of the method (see Sod [15] and [16], the normal velocity at the edge of the boundary layer was computed using equation (7b). This normal velocity at the edge of the boundary layer at $i\Delta z$ became the normal velocity at the edge of the interior calculation at $i\Delta z$. The result was at the end of a two-stroke cycle where the boundary layer equations were solved on a time scale 50 times greater than that of the interior, there were about 6500 vortex sheets. Despite the number of interactions between vortex sheets being small, this was still costly both in computer time and computer storage. Another serious drawback to this approach was that the boundary layer equations are no longer valid in the region where the boundary layer separates.

A method is introduced that brings the effect of the viscosity from the boundary into the interior in a more natural manner in such a way that most of the vortex sheets are not retained. See also Sod [4], [9], and [17].

Consider the Navier-Stokes equations for a viscous, incompressible fluid in an axially symmetric geometry in vorticity transport form

$$\partial_t \xi + (\underline{u} \cdot \underline{\nabla})\xi = \nu\Delta\xi + \frac{\nu}{r}\partial_r\xi - \frac{\nu}{r^2}\xi, \tag{11a}$$

$$\partial_r(ru_r) + \partial_z(ru_z) = 0, \tag{11b}$$

$$\xi \doteq \partial_z u_r - \partial_r u_z \tag{11c}$$

We can define the stream function ψ such that

$$u_r = -\frac{1}{r}\partial_z\psi \text{ and } u_z = \frac{1}{r}\partial_r\psi. \tag{12}$$

Consider a collection of N circular vortex filaments in $\mathbb{R}^3$ of intensity ξ_j which lie in a plane normal to the z-axis. This represents a point vortex in an axially-symmetric geometry in $\mathbb{R}^2$.

Under these conditions, we have for the j-th vortex filament with center $\underline{r}_j = (r_j, z_j)$

$$\psi_0(\underline{r} - \underline{r}_j) = -\frac{\xi_j(r - r_j)r_j}{8\pi}\int_0^\infty e^{-k|z-z_j|}J_1(k(r - r_j))J_0(kr_j)\,dk \tag{13}$$

where J_0 and J_1 are Bessel functions of the first kind of order zero and one respectively.

The vortcity field is given by $$\xi(\underline{r}) = \sum_{j=1}^{N} \xi_j \xi_0(\underline{r} - \underline{r}_j)$$

where $$\xi_0(\underline{r}) = \begin{cases} \dfrac{1}{4\pi\sigma||\underline{r}||}, & ||\underline{r}|| < \sigma, \\ 0, & ||\underline{r}|| \geq \sigma, \end{cases} \tag{14}$$

and σ is a cut-off which is taken to be $h/2\pi$. It is seen that ξ_0 is a smooth approximation to be Dirac delta function.

The vortex blob $\xi_0(\underline{r})$ generates its own stream function $\psi(\underline{r})$ which may be obtained by solving

$$\Delta\psi_0 - \frac{1}{r}\partial_r\psi = - r\xi_0.$$

Since σ is small we see that for $||\underline{r} - \underline{r}_j|| < \sigma$, r is near r_j (the r-coordinate of the j-th vortex blob which is the radius of the j-th vortex filament in $\mathbb{R}^3$) as a result we replace $\frac{1}{r}$ in(12) with $\frac{1}{r_j}$. This gives a new relationship between the stream function and the vorticity

$$\Delta\psi_0 = -r\,\xi_0 \quad ,$$

which has solution

$$\psi_0(\underline{r} - \underline{r}_j) = \frac{r_j}{4\pi\sigma}||\underline{r} - \underline{r}_j||.$$

Combining this with (13) gives the stream function $\psi_0(\underline{r} - \underline{r}_j)$ generated by (14). Furthermore, it is possible to generate a velocity field $\underline{v}(\underline{r} - \underline{r}_j)$ induced by this vorticity field,

$$\underline{v}(\underline{r}) = \sum_{j=1}^{N} \xi_j \underline{v}_0(\underline{r} - \underline{r}_j) \quad ,$$

where $v_0(\underline{r} - \underline{r}_j)$ is the velocity field at $\underline{r}$ induced by a single vortex blob located at $\underline{r}_j$. By differentiating the stream function $\psi_0(\underline{r} - \underline{r}_j)$ we obtain

$$\underline{v}_0(\underline{r} - \underline{r}_j) = \begin{cases} \left(-\frac{1}{r_j}\,\partial_z\psi_0(\underline{r} - \underline{r}_j), \frac{1}{r_j}\,\partial_r\psi_0(\underline{r} - \underline{r}_j)\right), & ||\underline{r} - \underline{r}_j|| < \sigma, \\ \left(-\frac{1}{r}\,\partial_z\psi_0(\underline{r} - \underline{r}_j), \frac{1}{r}\,\partial_r\psi_0(\underline{r} - \underline{r}_j)\right), & ||\underline{r} - \underline{r}_j|| \geq \sigma. \end{cases}$$

We are now in a position to describe the coupling of the boundary layer calculation to the interior calculation using the vortex filaments and the way in which the vortex sheets are removed.

The vortex sheets and vortex filaments are very similar in structure, that is, they are determined by their position and intensity. A segment of a vortex sheet with negative intensity will slow the fluid in the portion of the strip below it. Through the equation of conservation of mass (6b) we see that this negative intensity will create an upward flow to the left and a downward flow to the right similar to an actual vortex. The circulation around a vortex sheet of intensity ξ is ξh where h is the length of the sheet. The intensity of a vortex blob must be ξh, which gives a transition from vortex sheets to the vortex filaments. When a vortex sheet is converted to a vortex filament, its intensity ξ is multiplied by h, the length of the sheet.

Even in separated flow there is a thin viscous sublayer near the boundary where the boundary layer equations remain valid. This is an essential fact. For this allows us to use the vortex sheets near the boundary. The vortex sheets will satisfy the boundary conditions much more accurately than the vortex filaments. See Chorin, Hughes, McCracken, and Marsden [18].

Let L be a length chosen in such a way that $P[|\eta|>L] < \varepsilon$, where ϵ is some small number. Using Tscebysheff's theorem (see Loéve [19], we see that L will be a multiple of the standard deviation $\sqrt{2\nu\Delta t}$. Any vortex sheet which is greater than a distance 2L from the boundary will be converted to a vortex filament by multiplying the intensity of the sheet by its lengths.

The velocity field induced by these vortex filaments on the interior grid is then computed using (14) where the integrals are computed using Gauss-Laguerre quadrature. This velocity field is added to the velocity field obtained by the interior calculation. Once this is done the vortex filaments are destroyed. This This leaves only a small number of vortex sheets at any given time.

This approach is consistent with what happens physically for a slightly viscous flow. Far away from the boundaries the flow may be considered inviscid. The vorticity brought into the interior using the vortex filaments is advected with the flow through the interior method.

4. Application to a Motored Engine Chamber. The method is applied to a motored engine chamber, i.e., one that is driven externally. The engine is assumed to be axially symmetric, with a single intake-exhaust valve located on the chamber axis. The piston motion and valve timing represent an engine timing of 2500 RPM. The bore to stroke ratio is 1, the compression ratio is 0.6, and the Reynolds number for the boundary layer calculation is 10^4. The intake part is maintained at a constant pressure of 1 atmosphere and a temperature of 800^0F. Where the piston is at bottom dead center (the position where the piston is furtherest from the head of the cylinder) the cylinder and the intake-exhaust port lie in a 20 x 56 fixed (Eulerian) grid.

As a result of using the circular vortex filaments, the average number of sheets retained at any one time step is 300. This brings about a considerable savings in computer time and storage.

Figures 1 and 2 are vector plots of the velocity field for every other computational grid point. For each plot the vectors are scaled linearly with the

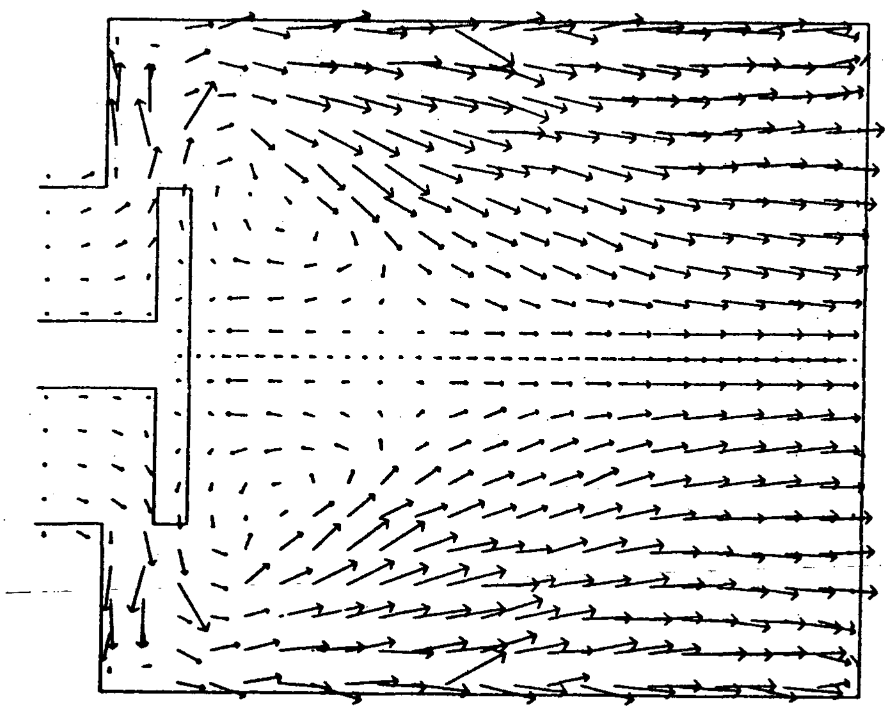

Figure 1 – Velocity field plot prior to completion of intake stroke depicting toroidal vortex at valve lip

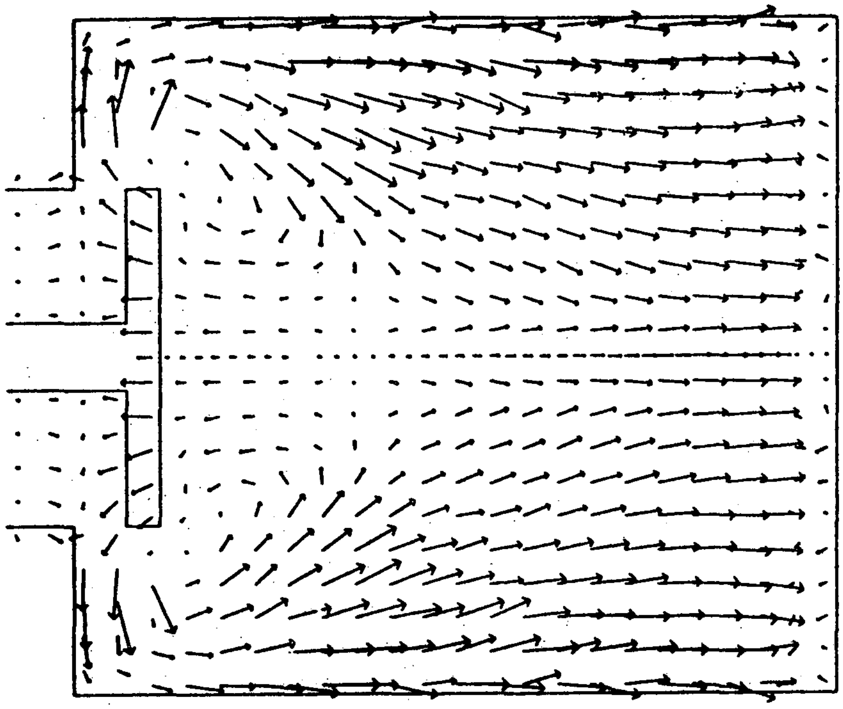

Figure 2. Velocity field plot at beginning of compression stroke depicting closing of valve and the stretching of vortex.

longest vector being twice the maximum velocity. These plots are just prior to the end of the intake stroke and just after the beginning of the compression stroke. The toriodal vortex which is formed during the intake stroke is stretched during the closing of the valve during the compression stroke.

5. Conclusions. **Until such time as useful experimental measurements of the flow in** the cylinder of an internal combustion engine can be made, an assessment of the accuracy of this computation cannot be made. Work is beginning in this area. Laser schlieren photographs of the flow in a cylinder are being taken by A. K. Oppenheim. Hot-wire measure-ments at one point in the flow field of a motored engine have been taken by Witze [20]. The results depicted in Figures 1 and 2 are in reasonable agreement with the experimental location and structure of the large vortex shed from the valve lip obtained by A. Ekchain and D. Hoult [21]. However, these experiments where performed with an incompressible fluid (water) whereas the fluid used in the numerical model was compressible.

A random moving grid method in the spirit of Glimm's method has been implemented which in the case of a motored engine chamber gives much better revolution when the piston approaches top dead center.

The method of solution is being generalized to a variable geometry. See Sod [22]. In the application to a motored engine chamber this gives rise to allowing a curved piston head, curved valve head, and a beviled edged on the valve and valve seat in the intake part. The main advantage of the method is that all of the boundary conditions (including piston and valve motion) from the interior method can be built into the boundary layer calculation. This will eliminate the problem caused by imposing the boundary condition on the interior method when the boundary is oblique to the mesh. The cost of this improvement will be a minor amount of extra work required to couple the interior and boundary layer methods.

6. References.

[1] G. A. Sod, J. Fluid Mech., 83, 785(1977).

[2] _________, "A Study of Cylindrical Implosion," Lectures on Combustion Theory, Samuel Z. Burstein, Peter D. Lax, and Gary A. Sod, editors, Department of Energy Research and Development Report COO-3077-153, New York University, (1978).

[3] A. J. Chorin, J. Comp. Phys., 27, 428(1978).

[4] G. A. Sod, A Random Approximation to a Boundary Layer Exhibiting Separation and Reattachment, to appear.

[5] J. Glimm, Comm. Pure Appl. Math., 18, 697(1965).

[6] A. J. Chorin, J. Comp. Phys., 22, 517(1976).

[7] S. K. Godunov, Mat. Sboruik, 47, 271(1959).

[8] A. J. Chorin, J. Comp. Phys., 27, 1(1978).

[9] G. A. Sod, "A Numerical Method for Slightly Viscous Axi-symmetric Flows with Application to Internal Combustion Engines," J. Comp. Phys., to appear. Preprint: Lawrence Berkeley Laboratory Report LBL-9049, (1979).

[10] P. Colella, "The Effects of Sampling and Operator Splitting on the Accuracy of the Glimm Scheme," Ph.D. Thesis, University of California, Department of Mathematics, Berkeley (1978).

[11] A. Lapidus, J. Comp. Phys., 2, 154(1967).

[12] G. A. Sod, Numerical Methods in Fluid Dynamics, Academic Press, to appear.

[13] H. Schlichtling, Boundary Layer theory, 6th Ed., McGraw-Hill, Inc., New York, (1968).

[14] A. J. Chorin, J. Fluid Mech., 57, 785(1973).

[15] G. A. Sod, "Automotive Engine Modeling with a Hybrid Random Choice Method," SAE paper 790242, (1979).

[16] G. A. Sod, "A Hybrid Random Choice Method with Application to Internal Combustion Engines," Proceedings Sixth International Conference on Numerical Methods in Fluid Dynamics, Springer-Verlag, 1978.

[17] G. A. Sod, "A Hybrid Random Choice Method with Applications to Automotive Engine Modeling," Proceedings of the Third IMACS International Symposium on Computer Methods for Partial Differential Equations, Bethlehem, Pennsylvania, (1979).

[18] A. J. Chorin, Huges, T. J. R., McCracken, M. T., and Marsden, J. R., Comm. Pure Appl. Math., 31, 205(1978).

[19] M. Loéve, Probability Theory, 2nd Ed., Princeton University Press, D. Van Nostrand (1960).

[20] P. O. Witze, "Hot-Wire Measurements of the Turbulence Structure in a Motored Spark-Ignition Engine," Sandia Laboratories Report SAND75-8697, Livermore, California (1976).

[21] A. Ekchain and Holt, P., "Flow Visualization Study of the Intake Process of an Internal Combustion Engine," SAE Paper 79005, (1979).

[22] G. A. Sod, "A Numerical Method for Axi-symmetric Flow in a Variable Geometry with Application to Internal combustion Engines," to appear.

TECHNICAL INFORMATION DEPARTMENT
LAWRENCE BERKELEY LABORATORY
UNIVERSITY OF CALIFORNIA
BERKELEY, CALIFORNIA 94720